



iJRASET

International Journal For Research in
Applied Science and Engineering Technology



INTERNATIONAL JOURNAL FOR RESEARCH

IN APPLIED SCIENCE & ENGINEERING TECHNOLOGY

Volume: 8 Issue: VI Month of publication: June 2020

DOI: <http://doi.org/10.22214/ijraset.2020.6341>

www.ijraset.com

Call:  08813907089

E-mail ID: ijraset@gmail.com

A ZVT-ZCT PWM Multiphase Synchronous Buck Converter with an Active Auxiliary Circuit for Low Voltage High Current Applications

S Shiva Kumar¹, P Prasanth Kumar²

¹Department of Electrical Engineering, Birla Institute of Technology, Mesra, Ranchi, India

²Department of Electrical and Electronics Engineering, Gokaraju Rangraju Institute of Engineering and Technology, Hyderabad, Telangana, India

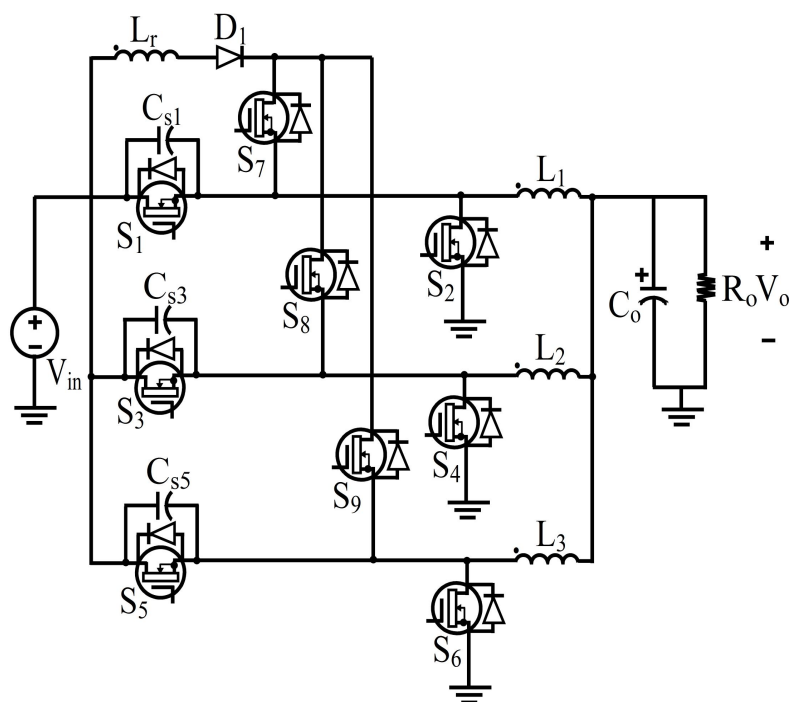
Abstract: In this paper, a Zero Voltage Transition (ZVT) – Zero current Transition (ZCT) Pulse-width Modulated (PWM) multiphase synchronous buck converter (SBC), with an active auxiliary circuit is proposed, that reduces the stresses and enhances the efficiency abating the switching and conduction losses of the converter. The important design feature of ZVT-PWM multiphase SBC converters is placement of resonant components that pacifies the switching and conduction losses. Due to the ZVT-ZCT, the resonant components with low values are used that results in the increase of switching frequency. High current multiphase buck converters found applications in advanced data control, solid state lasers, communication equipment and Pentium processors etc. The zero-voltage-transition and zero current transition operation of the proposed converter is presented through theoretical analysis. A simple design method for auxiliary circuit is discussed. The characteristics of the proposed converter are verified with the simulation in the PSIM cosimulated with MATLAB/SIMULINK environment and validated with experimental results.

Index Terms: Zero Voltage Transition (ZVT), Zero Current Transition (ZCT), Multiphase synchronous buck converter, pulse width modulation (PWM).

I. INTRODUCTION

In the recent times, the ZVT-ZCT technique applied to SBC facilitates reduction of switching losses, while maintaining voltage and current stresses within the tolerable limit. The ZVT-ZCT concept extending to multiphase SBC has emerged as a leading candidate for meeting the power requirement of the portable electronic systems. High current multiphase buck converters (MBC) are used in computing, graphics, and telecom applications. To achieve high power-density converters and high-performance, the switching frequency of the converters need to be increased. The traditional hard switching pulse-width-modulation (PWM) converters operating at high frequency is limited because of substantial switching loss. A few soft-switching technologies have been proposed to reduce switching loss and most of the new soft-switching converters reduce switching loss only at the expense of much increased voltage/current stresses of the switches, which increases the conduction loss. A new family of zero-voltage-transition (ZVT) PWM converters was presented [1] and widely used in the industry [2]. The concept of ZVT was also extended to full-bridge PWM converters [3], [4]. In these converters, the zero-voltage switching condition which is bestowed by auxiliary circuit for wide line and load ranges provides minimum voltage and current stresses on devices. Another way to achieve high-performance and high-power density converters is adopting the multiphase conversion technique [5]–[8]. With the interleaved operation, small size inductors can be used keeping low current ripple at the input and output capacitor filters, and high dynamic performance can be achieved since the operating frequency of input and output filter capacitors is increased by n times for n -phase converters. Higher dynamic performance and higher power-density power conversion can be achieved if both ZVT-ZCT and multiphase conversion techniques are combined. With a duty cycle of less than 10 %, raising the switching frequency to multi-MHz level will reduce the efficiency to less than 80 %. Because the switching frequency is equal to the inductor current ripple frequency, the switching frequency is limited between 300 kHz to 500 kHz [9-14]. When the inductor current slew rate is increased with a smaller inductance value to improve the transient response, then the inductor current ripple also increases. It is not only a harmful action for the high-side switch due to larger turn-off loss, but also for the low-side switch due to a larger conduction loss. It also increases the inductor winding losses. This conflict limits the average inductor current in each channel [15-20]. Moreover, there is a tradeoff between efficiency and transient response. As a result, these technical conflicts do not only increase the costs and sacrifice the power density, but also difficultly meet the power requirements of future microprocessors before the technical conflicts are resolved [21-23].

In this paper, the ZVT-ZCT multiphase synchronous buck converter is presented with the directive to improve its performance and alleviate the issues of conventional multiphase synchronous buck converter like unbalance distribution of current and high amount of losses in the converter. The proposed converter achieves ZVS and ZCS with reduction in voltage and current stresses across switches to improve the efficiency by minimizing the switching and conduction losses with a simple active auxiliary circuit. Here the proposed multiphase is associated with active auxiliary circuit rather than passive auxiliary circuit because at high load current passive auxiliary circuit will give high conduction losses. Section I presents a description of the proposed topology. Principles of operations and its analysis are discussed in section II. Section III provides the design process of the multiphase converter. The predicted operation principles and the theoretical analysis of the converter are verified in section-IV with simulation results and experimental results in section-V.



II. OPERATING PRINCIPLE

In order to analyze the steady-state operations of the proposed circuit, the following assumptions are made during one switching cycle.

- 1) The input voltage V_{in} is constant.
- 2) The output current I_o is constant, or the output capacitor C_o is large enough.
- 3) The output Inductors L_1, L_2, L_3 is much larger than the resonant circuit inductor L_r .
- 4) The resonant circuits are ideal.
- 5) The reverse recovery time of diode is ignored.
- 6) The semiconductor devices are ideal.

B. Modes of Operation

Based on these assumptions, circuit operations in one switching cycle can be divided into fifteen stages. The key waveforms of these stages are illustrated in Fig.2 and the equivalent circuit schemes of the operation stages are given in Fig.3. The detailed analysis of every stage is presented below:

1) *Mode 1 (t0-t1)*: Prior to $t = t_0$, the body diode of switch S2 was conducting while the main switch S1 is off. The equations are $i_S = 0$, $i_{Ds2} = I_0/3$, $i_{Lr} = 0$, are valid at the beginning of this stage.

At $t = t_0$, the auxiliary switch S7 is turned on, which realizes zero-current turn-on as it is in series with the resonant inductor L_r . During this stage, i_{Lr} rises and current i_{Ds2} through body diode of switch S1 falls simultaneously at the same rate. The resonance occurs between L_r and C_{s1} .

This mode ends at $t = t_1$, when i_{Lr} reaches $I_0/3$, and i_{D4} becomes zero. The body diode of switch S4 is turned off with ZCS. The resonant current through inductor L_r is given by

$$i_{\text{resonant}}(t) = \frac{C_{s1} V_{Cs1} \omega \sin \omega t}{Z_1} \quad (1)$$

$$i_{Lr}(t) = \frac{V_i}{L_r} \times t \quad (2)$$

Where

$$\omega = \frac{1}{\sqrt{L_r C_{s1}}}, \quad Z_1 = \sqrt{\frac{L_r}{C_{s1}}}$$

At

$$t = t_1, \quad i_{Lr}(t) = \frac{I_o}{3},$$

Therefore,

$$t_{01} = t_1 - t_0 = \frac{I_o L_r}{3 V_{in}}.$$

2) *Mode 2(t1-t2)*: Since the inductor current i_{Lr} is increasing continuously beyond one third of load current, the exceeding current makes the diode DS1 to conduct. At $t = t_1$, $i_{S7} = i_{Lr} = I_0/3$. After reaching the peak current I_{Lrmax} , the inductor current starts decreasing. This mode comes to an end when i_{Lr} becomes again equal to $I_0/3$. At this moment, the main switch is triggered to turn on under zero voltage switching (ZVS). The discharge current of capacitor C_{s1} through the body diode having a resistance R is given as:

$$i_{C_{s1}} = \frac{V_{Cs1}}{R} e^{-t/R C_{s1}} \quad (3)$$

$$i_{Lr}(t) = \left(i_{Lrmax} - \frac{I_o}{3} \right) e^{-\frac{t - t_1}{R}} \quad (4)$$

At

$$t = t_2, \quad i_{Lr}(t) = \frac{I_o}{3},$$

Therefore,

$$t_{12} = t_2 - t_1 = \frac{2R}{L_r} \ln \frac{3 I_{Lrmax}}{I_0}.$$

3) *Mode 3(t2-t3)*: At $t = t_2$, the main switch is turned on while the auxiliary switch is still in on state. Now the stored energy in inductor L_r will be transferred to the load at the same rate as the current increase through the main switch S1. At $t = t_2$, $i_{Lr} = I_0/3$.

This mode comes to end when the total energy of the resonant inductor will be transferred to the load. The auxiliary switch S7 will turn off under ZCS.

The inductor current i_{Lr} during this mode can be expressed as:

$$i_{Lr}(t) = I_{Lr \max} e^{-t/L_r/R_{on}} \quad (5)$$

$$i_{s1} + i_{Lr} = I_0/3 \quad (6)$$

At the end of this mode, at $t = t_3$.

$$i_{s1} = I_o / 3 \quad (7)$$

$$i_{Lr} = 0 \quad (8)$$

Therefore,

$$t_{23} = t_3 - t_2 = \frac{2R_{on}}{L_r} \ln \frac{3I_{Lr \max}}{I_0}$$

4) *Mode 4(t3-t4):* In this mode, the converter behaves as a conventional PWM converter. For the required output voltage, the turn on period of the main switch is decided. At the end of this mode, the main switch S1 is turned off under ZVS due to the existent of capacitor CS1 across it. The current expression for this mode can be expressed as:

$$i_{s1} = I_0/3 \quad (9)$$

5) *Mode 5(t4-t5):* At $t = t_4$, the synchronous switch is turned on to provide a constant load current. At the end of this mode, the complete operation for one phase converter is completed and the second auxiliary switch S8 is turned on with a phase difference of $360/n$, where n is the number of phases, here $n=3$. The same five modes will be repeated for each phase. So there are fifteen modes for this proposed multiphase converter. The current expression for this mode can be expressed as:

$$i_{s2} = I_o / 3 \quad (10)$$

$$i_{Cs1} = \frac{V_{Cs1}}{R} e^{-t/RC_{s1}}$$

At the end of this mode, at $t = t_5$,

$$i_{Cs1} = 0$$

Therefore,

$$t_{45} = t_5 - t_4 = RC_{s1} \ln \frac{V_{Cs1}}{RC_{s1}}$$

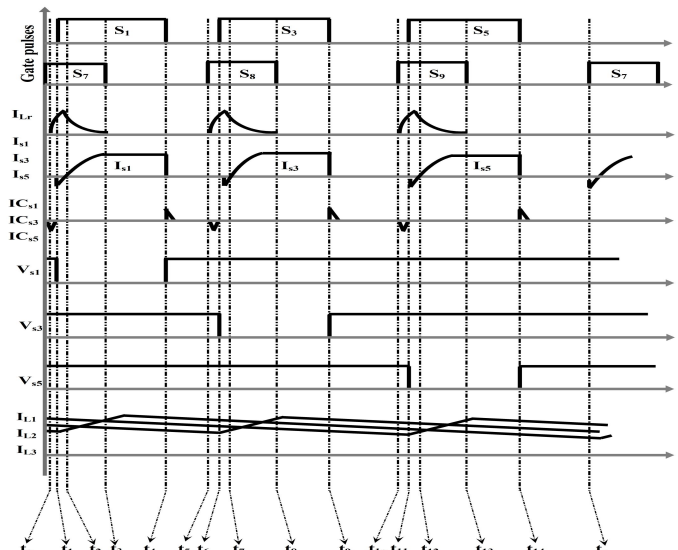


Fig.2: Key waveforms of the proposed ZVT-ZCT multiphase synchronous buck converter.

C. Output Voltage

The output voltage can be evaluated by balancing the volt-second relationship or by equating the energy relation i.e.,

$$V_o \tau = 3V_{in} [t_{01} + t_{12} + t_{23} + t_{34} + t_{45}]$$

$$V_o \tau = 3V_{in} \left[\frac{I_0 L_r}{3V_{in}} + \frac{2R}{L_r} \ln \frac{3I_{Lrmax}}{I_0} + \frac{2R_{on}}{L_r} \ln \frac{3I_{Lrmax}}{I_0} + RC_{S1} \ln \frac{V_{CS1}}{RC_{S1}} \right] \quad (11)$$

Where

$$\tau = \frac{1}{f_s} \quad \text{And } f_s = \text{Switching frequency.}$$

From the above expression, it is noticeable that voltage conversion ratio depends upon switching frequency irrespective of the duty ratio.

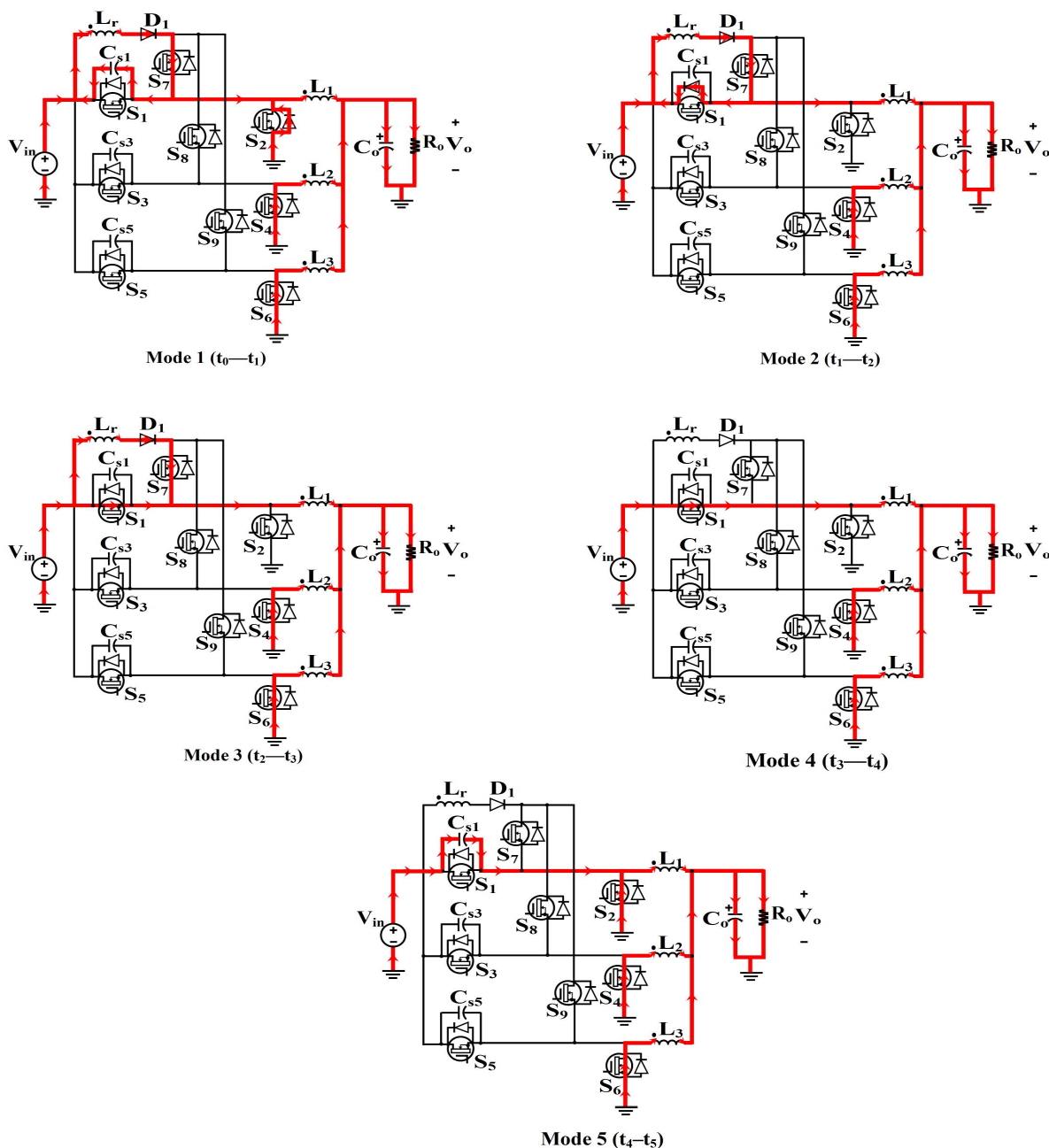


Fig.3: Operational modes of the proposed ZVT multiphase synchronous buck converter

III. DESIGN PROCEDURE OF AUXILIARY CIRCUIT COMPONENTS

The design procedure of auxiliary component is as follows:

Resonant capacitor CS1 is selected to discharge from V_{in} to zero with the maximum output current over at least the time period t_{on} during the turn on of body diode. For this state, according to equations (3)

$$RC_{S1} \ln \frac{RI_0}{V_{CS1}} \geq t_{on} \quad (12)$$

Resonant inductor L_r is selected such that current through inductor can be reduced to zero from $I_o/3$ in the same duration of rise in current from zero to $I_o/3$ in main switch.

In this case, we get from equation (5).

$$t_{23} = \frac{R_{on}}{L_r} \quad (13)$$

IV. SIMULATION RESULTS

The converter is simulated using simulation software PSIM version 7.1 co-simulated with MATLAB/Simulink. The proposed converter works with an input voltage of $V_{in}=12V$ and an output voltage of $V_o=1V$, a load current of 100A and a switching frequency of $f_s=500kHz$. Fig. 4(a)–(e) shows the simulation results of the proposed converter.

Fig. 4 (a) – 4(c) shows the voltage and current waveforms of the main, synchronous and auxiliary switches in the proposed ZVT-ZCT PWM SBC. Fig 4 (d) presents the current waveform of resonant inductor L_r and fig. 4 (e) shows the currents through filter inductors L_1 , L_2 , L_3 . The above simulation results of main, synchronous and auxiliary switches substantiate that the voltage and current stresses are extremely low. The uniform current distribution in each phase which is a major problem in a multiphase synchronous buck converter is elucidated in the proposed converter.

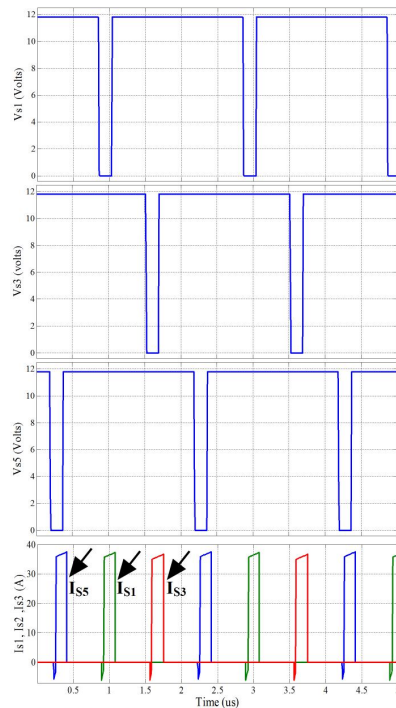


Fig. 4 (a) Voltage and current waveforms of switch S_1, S_2, S_3 : V_{s1}, V_{s2}, V_{s3} and I_{s1}, I_{s2}, I_{s3} .

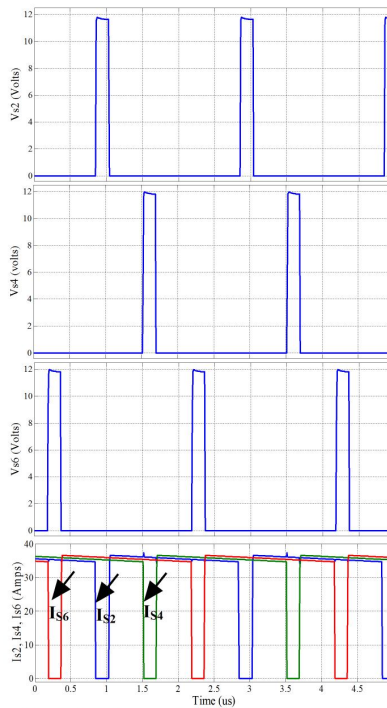


Fig. 4 (b) Voltage and current waveforms of switch S_2, S_4, S_6 : V_{s2}, V_{s4}, V_{s6} and I_{s2}, I_{s4}, I_{s6} .

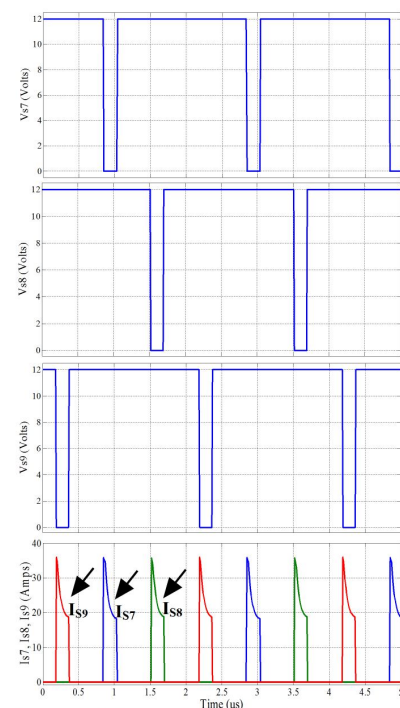


Fig. 4 (c) Voltage and current waveforms of switch S_7, S_8, S_9 : V_{s7}, V_{s8}, V_{s9} and I_{s7}, I_{s8}, I_{s9} .

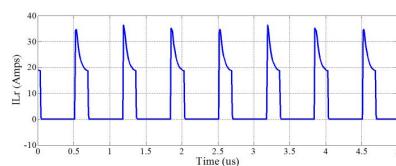


Fig. 4 (d) Current waveform of inductor L_r : I_{Lr}

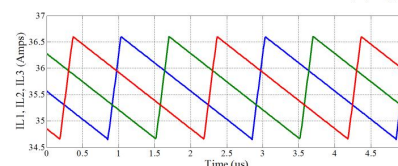


Fig. 4 (e) Current waveforms of inductors L_1, L_2, L_3 : I_{L1}, I_{L2}, I_{L3} .

Fig 4: Voltage and Current Waveforms

V. EXPERIMENTAL RESULTS

The multiphase ZVT-ZCT PWM synchronous buck converter integrated with active auxiliary circuit has been built and substantiated with experimental results. Experimental results shown in Fig. 5 depicts analogous to the simulation results. The Fig. 5 (a) shows the voltage and current waveforms of main switches S1, S3, S5 wherein the voltage and current stresses on the main switches are imperceptible. The Fig. 5 (b) presents the voltage and current waveforms of synchronous switches S2, S4, S6 which shows minimal voltage and current stresses. Similarly Fig. 5 (c) corroborates that the voltage and current stresses on auxiliary switches S7, S8, S9 are eliminated. The Fig. 5 (d) presents the current waveform of resonant inductor L_r and Fig. 5 (e) depicts that the current through the filter inductors L1, L2, L3 in each phase uniformly distributed that solves the issue of phase shedding. The experimental components employed in the proposed converter are tabulated in Table 1.

Table 1: COMPONENTS USED FOR PROPOSED CONVERTER

Component	Experimental Value/Model
Main Switches, S1, S2, S3	IRLR8721PbF
Synchronous Switches, S4, S5, S6	IRLR8721PbF
Auxiliary Switches, S7, S8, S9	IRLR8721PbF
Diode D1	MBRB4030
Resonant Inductor, L_r	22 nH
Capacitors Cs1, Cs2, Cs3	4.7 nF
Output Capacitor, C_o	20 μ F
Output Inductor, L1, L2, L3	2 μ H

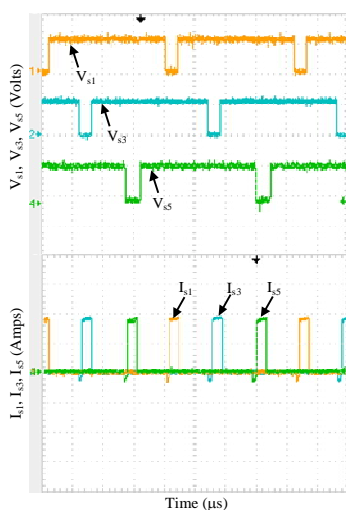


Fig. 5 (a) Experimental Voltage and current waveforms of main switches S1, S3, S5 [V_{s1}, V_{s3}, V_{s5}: 12V/Div; I_{s1}, I_{s3}, I_{s5}: 17.5A/Div; time: 0.5 μ s/Div]

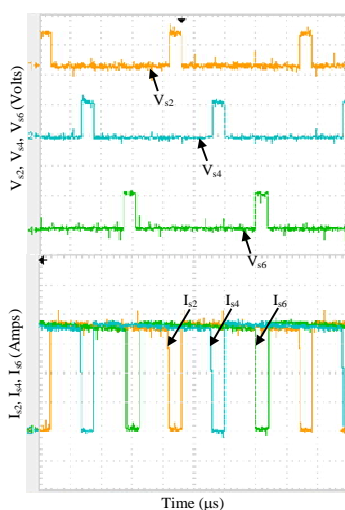


Fig. 5 (b) Experimental Voltage and current waveforms of synchronous switches S2, S4, S6 [V_{s2}, V_{s4}, V_{s6}: 12V/Div; I_{s2}, I_{s4}, I_{s6}: 17.5A/Div; time: 0.5 μ s/Div]

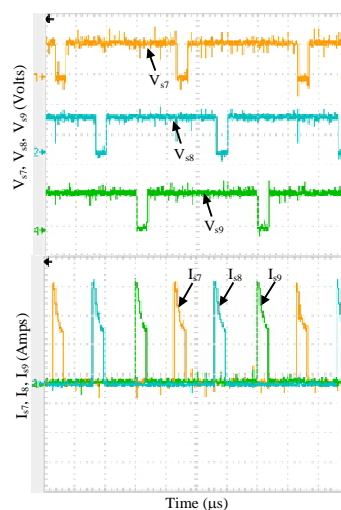


Fig. 5 (c) Experimental Voltage and current waveforms of auxiliary switches S7, S8, S9 [V_{s7}, V_{s8}, V_{s9}: 12V/Div; I_{s7}, I_{s8}, I_{s9}: 17.5A/Div; time: 0.5 μ s/Div]

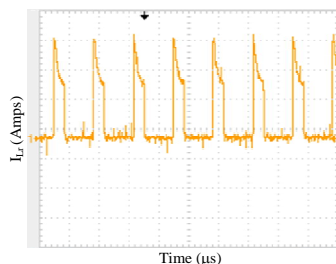


Fig. 5 (d) Experimental current waveforms of resonant inductor L_r [I_{Lr}: 10A/Div; time: 0.5 μ s/Div]

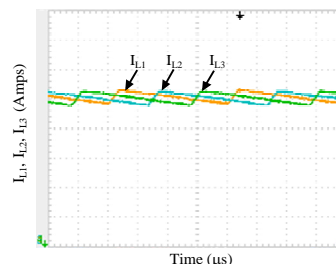


Fig. 5 (e) Experimental current waveforms of filter inductors L1, L2, L3 [I_{L1}, I_{L2}, I_{L3}: 7A/Div; time: 0.5 μ s/Div]

Fig 5: Experimental Voltage and Current waveforms

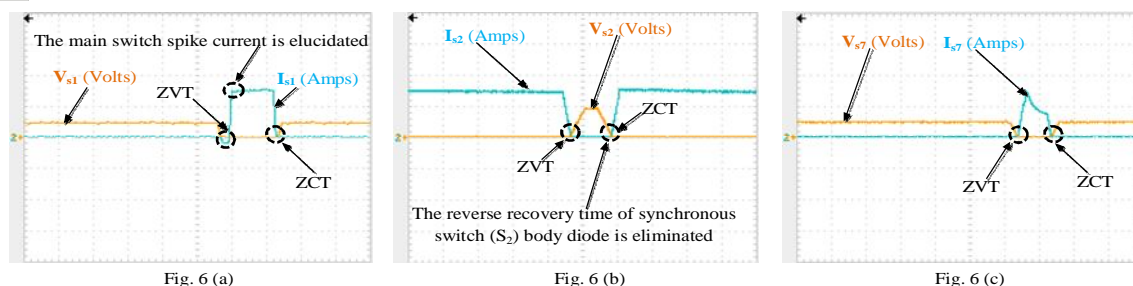


Fig. 6 Experimental voltage and current waveforms of:

6 (a) Main switch (S_1): [V_{S1} : 24V/Div, i_{S1} : 20A/Div, time: 0.2 μ s/Div]

6 (b) Synchronous switch (S_2): [V_{S2} : 24V/Div, i_{S2} : 20A/Div, time: 0.2 μ s/Div]

6 (c) Auxiliary switch (S_7): [V_{S7} : 24V/Div, i_{S7} : 20A/Div, time: 0.2 μ s/Div], exemplifies ZVT turn ON and ZCT turn OFF of the switches in the proposed converter.

Fig 6: Experimental Voltage and Current waveforms

The Fig. 6 (a) signifies that the main switch S_1 spike current is plummeted; the waveform is almost equivalent to the traditional buck converter. Consequently, the rating of the main switch required for the buck converter is economized by the introduction of ZVT-ZCT operation. The main switch is turned ON under ZVT and turned OFF with ZCT, due to which the mainstream switching losses got diminished. Fig. 6 (b) the synchronous switch S_2 is turned OFF under ZCT and turned ON with ZVT operation. The reverse recovery (RR) effect due to the body diode of S_2 is almost attenuated. The auxiliary switch in Fig. 6 (c) is turned ON under ZVT and turned OFF with ZCT thereby reducing the voltage and current stresses on the switch. The Fig. 7 shows the experimental setup implementation of the proposed converter. The simulation and experimental results affirm that the component's voltage and current ratings, and also the energy volumes of passive elements used are considerably reduced that enhances the performance of the proposed converter.

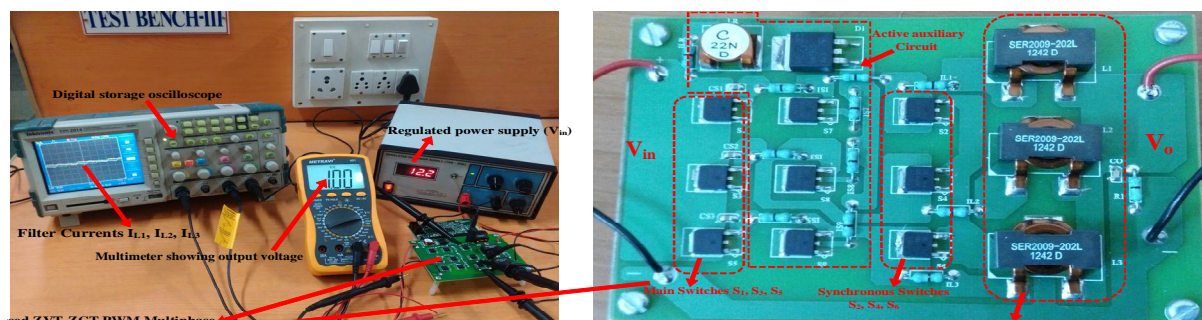


Fig 7: Experimental setup of Proposed ZVT-ZCT PWM multiphase synchronous Buck Converter

A. Efficiency Curve

From Fig. 8, efficiency values of the proposed converter are comparatively higher than the traditional converter. The converter is designed for the maximum output current, and it is accustomed that towards minimum output power efficiency, values decrease. At nearly 70A of output current, the efficiency of the proposed converter rises to about 96% when compared to the counterpart traditional converter whose efficiency is about 87%. The high efficiency of the proposed converter proves the definiteness of the design values.

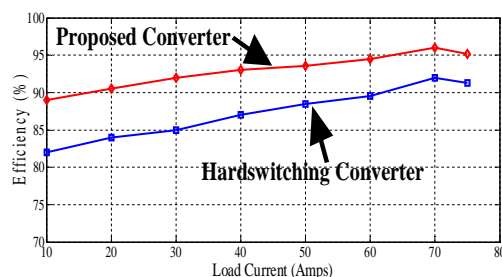


Fig 8: Efficiency curve

VI. CONCLUSION

In this paper, the concept of ZVT-ZCT is implemented in multiphase synchronous buck converter and it is shown that the switching losses in synchronous buck are eliminated. Significant efficiency improvement with soft switching as compared to hard switching converter is achieved and it is evident from the efficiency curve. Both main switch and synchronous switches are turned-on and turned-off under ZVS and ZCS, respectively. The auxiliary switches are turned-on and turned-off under ZVS and ZCS with tolerable voltage stresses across the switch. Hence switching losses are reduced and the proposed multiphase synchronous buck is highly efficient than the conventional converter. This proposed converter of high switching frequency is designed for application in new generation microprocessor.

REFERENCES

- [1] G. Hua, C. S. Leu, and F. C. Lee, "Novel zero voltage transition PWM converters," in Proc. IEEE PESC Rec. 1992, pp. 55–61.
- [2] G. Hua, W. A. Tabisz, C. S. Leu, N. Dai, R. Watson, and F. C. Lee, "Development of dc distributed power system components," in VPEC Annu. Seminar, 1993 Proc., pp. 87–96.
- [3] J. G. Cho and G. H. Cho, "Novel off-line zero-voltage switching PWM ac/dc converter for direct conversion from ac line to 48 VDC bus with power factor correction," in Proc. IEEE PESC Rec. 1993, pp. 689–695.
- [4] J. G. Cho, J. Sabat'e, and F. C. Lee, "Novel zero-voltage-transition PWM dc/dc converter for high power applications," in Proc. IEEE APEC Rec. 1994, pp. 143–149.
- [5] D. M. Sable, F. C. Lee, and B. H. Cho, "A zero-voltage-switching bidirectional battery charger & discharger for the NASA EOS satellite," in VPEC Annu. Seminar, 1992 Proc., pp. 41–46.
- [6] J. P. Noon, B. H. Cho, and F. C. Lee, "Design of multi-module multiphase battery charger for the NASA EOS space platform test bed," in VPEC Annu. Seminar, 1992 Proc., pp. 137–142.
- [7] C. Hua, W. A. Tabisz, C. S. Leu, N. Dai, R. Watson, and F. C. Lee, "Development of DC distributed power system components," in VPEC Annu. Seminar, 1992 Proc., pp. 137–142.
- [8] B. D. Bedford and R. G. Hoft, Principles of Inverter Circuits. New York: Wiley, 1964.
- [9] Panov Y., and Jovanovic M. M., "Design considerations for 12-V/1.5-V, 50-A voltage regulator modules," in IEEE Tran. on Power Electron., vol.16(6), pp. 776–783, Nov 2001.
- [10] Zhou X. W., Wog P., Lee F., "Investigation of candidate VRM topologies for future microprocessors," in IEEE Tran. on Power Electron., pp. 1172-1182, 2000.
- [11] T. Hegarty, "Benefits of multi-phasing buck converters," National Semiconductors.
- [12] Zhou X., Xu P., and Lee F. C., "A high power density, high frequency and fast transient voltage regulator module with a novel current sensing and current sharing technique," in Proceedings of IEEE APEC 1999, pp. 289–294.
- [13] Huang W., Schuellein G., and Clavette D., "A Scalable Multiphase Buck Converter with Average Current Share Bus," in Proceedings of IEEE APEC 2003, pp. 438-443.
- [14] Zhou X. W., Xu P., Lee F., "A novel current sharing control technique for low voltage high current voltage regulator module applications," in IEEE Tran. on Power Electron., pp. 1153-1162, 2000.
- [15] Eirea G., and Sanders S. R., "Phase Current Unbalance Estimation in Multiphase Buck Converters," in IEEE Tran. on Power Electron., vol. 23(1), pp. 137-143, January 2008.
- [16] García O., Zumel P., Castro A., Alou P., and Cobos J. A., "Current Self-balance Mechanism in Multiphase Buck Converter", Application note,
- [17] Gu W., Qiu W., Wu W., and Batarseh I., "A Multiphase DC/DC Converter with Hysteretic Voltage Control and Current Sharing", in Proceedings of IEEE APEC 2002, pp. 670-674.
- [18] Jakobsen L. T., Garcia O., Oliver J. A., Alou P., Cobos J. A. and Andersen M. A. E., "Interleaved Buck Converter with Variable Number of Active Phases and a Predictive Current Sharing Scheme", Application note,
- [19] Costabeber, A., Mattavelli, P., and Saggini, S., "Digital Time-Optimal Phase Shedding in Multiphase Buck Converters," in IEEE Tran. on Power Electron., vol. 25(9), pp. 2242-2247, September 2010.
- [20] Nagaraja H.N., Patra A., and Kastha D., "Design and analysis of four-phase synchronous buck converter for VRM applications," in Proceedings of the IEEE INDICON 2004.
- [21] Cho J.-G., Baek J.-W., Rim G.-H., and Kang I.; "Novel Zero-voltage-transition PWM Multiphase Converters," in IEEE Tran. on Power Electron., vol. 13(1), pp. 152-159, 1998.
- [22] Qiu Y., "High-Frequency Modeling and Analyses for Buck and Multiphase Buck Converters," Ph. D. Dissertation, 2005, Blacksburg, Virginia.
- [23] E. Adib, H. Farzanehfar, "Zero-voltage transition current-fed full-bridge PWM converter," IEEE Trans. Power Electron., vol. 24, no. 4, pp. 1041-1047, April. 2009.
- [24] H. L. Do, "A soft –switching DC/DC converter with high voltage gain," IEEE Trans. Power Electron., vol. 25, no. 5, pp. 1193-1200, May. 2010.
- [25] S. Pattnaik, A.K. Panda, K. K. Mahapatra, "Efficiency improvement of synchronous buck converter by passive auxiliary circuit," IEEE Trans. Industrial Appl., vol. 46, no. 6, pp. 2511 – 2517, Nov/Dec. 2010.
- [26] H. Bodur, S. Cetin, G. Yanik, "A new zero-voltage transition pulse width modulated boost converter," IET Power Electron., vol. 4, no. 7, pp. 827–834, August. 2011.
- [27] S. Urgun, "Zero-voltage transition–zero-current transition pulse width modulation DC–DC buck converter with zero-voltage switching–zero-current switching auxiliary circuit," IET Power Electron., vol. 5, no. 5, pp. 627–634, march. 2012.
- [28] Hong-Tzer Yang, Jian-Tang Liao, Xiang-Yu Cheng, "Zero-Voltage-Transition auxiliary circuit with dual resonant tank for DC–DC converters with synchronous rectification," IET power Electron., vol. 6, no. 6, pp. 1157-1164, July. 2013.



10.22214/IJRASET



45.98



IMPACT FACTOR:
7.129



IMPACT FACTOR:
7.429



INTERNATIONAL JOURNAL FOR RESEARCH

IN APPLIED SCIENCE & ENGINEERING TECHNOLOGY

Call : 08813907089  (24*7 Support on Whatsapp)